Holocene variability of bottom water hydrography on the Kara Sea shelf (Siberia) depicted in multiple single-valve analyses of stable isotopes in ostracods

Johannes Simstich[a,*], Vladimir Stanovoy[b], Dorothea Bauch[a], Helmut Erlenkeuser[c], Robert F. Spielhagen[a,d]

[a] *Leibniz Institute of Marine Sciences at Kiel University (IFM-GEOMAR), Wischhofstr. 1-3, 24148 Kiel, Germany*
[b] *Arctic and Antarctic Research Institute, Bering Street, 38, 199397 St. Petersburg, Russia*
[c] *Leibniz-Labor for Radiometric Dating and Stable Isotope Research, Christian-Albrechts-Universität, Olshausenstr. 40, 24118 Kiel, Germany*
[d] *Mainz Academy for Science and Literature, Germany*

Abstract

Ostracods secrete their valve calcite within a few hours or days, therefore, its isotopic composition records ambient environmental conditions of only a short time span. Hydrographic changes between the calcification of individuals lead to a corresponding range (max.−min.) in the isotope values when measuring several (≥ 5) single valves from a specific sediment sample. Analyses of living (stained) ostracods from the Kara Sea sediment surface revealed high ranges of >2‰ of $\delta^{18}O$ and $\delta^{13}C$ at low absolute levels ($\delta^{18}O$: < 3‰, $\delta^{13}C$: < −3‰) near the river estuaries of Ob and Yenisei and low ranges of ~ 1‰ at higher absolute levels ($\delta^{18}O$: 2–5.4‰, $\delta^{13}C$: −3‰ to −1.5‰) on the shelf and in submarine paleo-river channels. Comparison with a hydrographic data base and isotope measurements of bottom water samples shows that the average and the span of the ostracod-based isotope ranges closely mirror the long-term means and variabilities (standard deviation) of bottom water temperature and salinity. The bottom hydrography in the southern part of the Kara Sea shows strong response to the river discharge and its extreme seasonal and interannual variability. Less variable hydrographic conditions are indicative for deeper shelf areas to the north, but also for areas near the river estuaries along submarine paleo-river channels, which act as corridors for southward flowing cold and saline bottom water.

Isotope analyses on up to five single ostracod valves per sample in the lower section (8−7 cal. ka BP) of a sediment core north of Yenisei estuary revealed $\delta^{18}O$ and $\delta^{13}C$ values which on average are lower by 0.6‰ in both, $\delta^{18}O$ and $\delta^{13}C$, than in the upper core section (< 5 cal. ka BP). The isotope shifts illustrate the decreasing influence of isotopically light river water at the bottom as a result of the southward retreat of the Yenisei river mouth from the coring site due to global sea level rise. However, the ranges (max.−min.) in the single-valve $\delta^{18}O$ and $\delta^{13}C$ data of the individual core samples are similar in the upper and in the lower core section, although a higher hydrographic variability is expected prior to 7 cal. ka BP due to river proximity. This lack of variability indicates the southward flow of cold, saline water along a submarine paleo-river channel, formerly existing at the core location. Despite shallowing of the site due to sediment filling of the channel and isostatic uplift of the area, the

* Corresponding author. Present address: Department of Earth Sciences, University of Cambridge, Downing Street, Cambridge CB2 3EQ, UK. Fax: +44-1223-333-450.

E-mail address: jsim.3@esc.cam.ac.uk (J. Simstich).

hydrographic variability at the core location remained low during the Late Holocene, because the shallowing proceeded synchronously with the retreat of the river mouth due to the global sea level rise.

1. Introduction

Variability in atmosphere and ocean of the Arctic is largely governed by the decadal-scale Arctic Oscillation and a low-frequency oscillation with a periodicity of 60–80 years (Proshutinsky et al., 1999; Polyakov and Johnson, 2000). In the 1990s, both oscillations were in a positive mode and probably amplified climate-driven changes in the polar regions (Moritz et al., 2002). For example, river-monitoring data reveal that the average annual discharge of freshwater from Eurasian rivers to the Arctic shelf seas increased by 7% from 1936 to 1999 (Peterson et al., 2002). This increase is superimposed on an extremely high variability on seasonal and interannual time scales. Eighty percent of the annual discharge of the rivers Ob and Yenisei occurs during summer from June to September (Pavlov and Pfirman, 1995) and their discharge can differ interannually by 10–40% from the decadal mean (Semiletov et al., 2000). High seasonal and interannual changes in the supply of river water are a major characteristic of Arctic shelf seas.

Any change of the total freshwater supply has significant implications for the formation and altering of Arctic water masses on the shelf, which play a major role in the hydrography of the Arctic basin and, in turn, in the global thermohaline circulation (Alley, 1995). The amount of freshwater and its variability directly affect the potential of vertical mixing through the pycnocline (Sanders and Garvine, 2001), the strength of shelf bottom currents (Dmitrenko et al., 2001), the extent and location of sea ice formation (Dmitrenko et al., 1998), and the formation of dense brine waters (Winsor and Chapman, 2002). Also, freshwater-induced stratification has a profound influence on productivity (Olli et al., 2002) and therefore on global change through the carbon cycle (e.g. Scourse and Austin, 2002). The seasonal and interannual variability of the Arctic freshwater supply therefore is an important climate control mechanism and its changes through time are worth investigating in

greater detail in order to understand and predict climatic changes.

As a step towards climate reconstructions from fossil records, we present stable isotope measurements on modern ostracod shells obtained from surface sediments in the Kara Sea. The results provide a basis to reconstruct the Holocene paleoenvironment from ostracod shells in a gravity core. Ostracods are small (mostly ≤1 mm) bivalved crustaceans, which produce two carbonate valves with an isotopic composition that is controlled by temperature and the isotopic composition of the ambient water during the time of valve secretion. Ostracoda, in contrast to other benthic calcareous organisms, molt their exoskeleton during growth and secrete a new calcareous carapace within a very short time span, no longer than 2–3 days (Benson, 1961; Peypouquet et al., 1988). This almost instantaneous formation of the isotope signal provides means to study hydrographic variability, because it may pinpoint extreme conditions, while continually growing organisms like molluscs or foraminifera integrate over much longer time spans.

2. Materials and methods

2.1. Hydrographic data

Our analysis of thermohaline characteristics in the bottom water layer is based on hydrological data covering the period 1929–2001 and the area of 72–77°N and 70–95°E (Fig. 1). Most of these data were collected during summer expeditions (July–October) of the Arctic and Antarctic Research Institute (St. Petersburg, Russia). Numerous observations from joint Russian–Norwegian and Russian–German expeditions between 1993 and 2001 extend the data base. Deep-sea thermometers, electrical salinity meters and titration were used until 1990; since then temperature and salinity values are determined with the usual CTD-probes (Conductivity–Temperature–
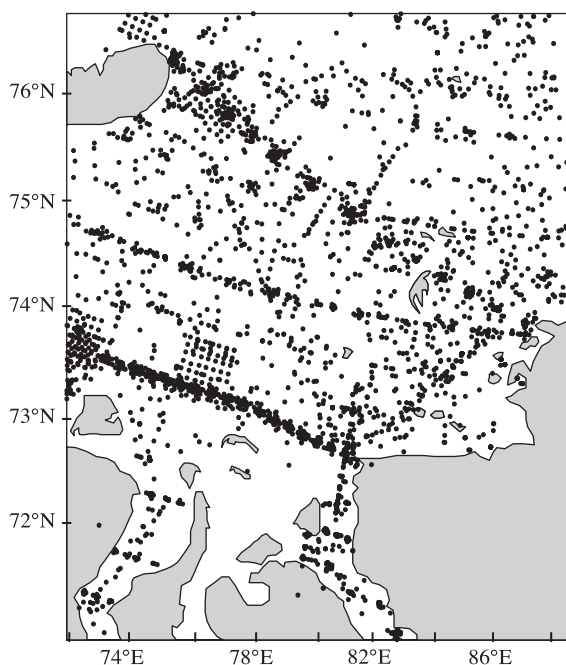
Fig. 1. Distribution of hydrographic stations used to extract mean summer temperature and salinity fields.

Depth). The analytical accuracy of all methods is equal to or better than 0.01–0.05 °C for temperature and 0.01 for salinity (Volkov et al., 2002). Salinity is reported without units using the Practical Salinity Scale (Millero, 1993).

In order to extract average temperature and salinity fields, only surveys which covered a large portion of the area were selected from the whole data set. The data of each of the 35 chosen surveys were interpolated by the Kriging method (e.g. Davis, 1986) on a grid with a resolution of 0.5° longitude and 0.25° latitude. Thereafter, average values for each grid point were calculated to obtain mean multiyear fields for the whole summer period.

2.2. Sample preparation and isotope measurements

2.2.1. Ostracods from sediment surface samples

In order to cover different ecological realms of the Kara Sea shelf, we analyzed four ostracod species of different salinity tolerance and water depth preference (Benson et al., 1983; Stepanova et al., 2003): the eurytopic species *Sarsicytheridea punctillata* (Brady, 1864), the euryhaline species *Hetero-*

cyprideis sorbyana (Jones, 1856) and *Paracyprideis pseudopunctillata* (Swain, 1963), and the brackish, shallow water species *Roundstonia macchesneyi* (Brady and Crosskey, 1871). Without in situ observations, microhabitat preferences of these species can be deduced only from the morphology of their carapaces. The ventral flattening and the rather smooth surface with little ornamentation may indicate species able to burrow in the upper few cm of the sediment (Benson, 1961). Shells of endobenthic animals often bear a stable carbon isotope composition ($^{13}C/^{12}C$) which is systematically lower than the $^{13}C/^{12}C$ signal of dissolved inorganic carbon in the bottom water (e.g. McCorkle et al., 1997) as result of the incorporation of pore water carbon, which is ^{13}C-depleted due to bacterial decay of organic matter in the sediment. Oxygen isotopes, on the other hand, are not affected by this process (McCorkle et al., 1997).

The analyzed samples were obtained during four summer expeditions to the Kara Sea between 1997 and 2001 (Matthiessen and Stepanets, 1998; Stein and Stepanets, 2000, 2001, 2002). Sediment samples were taken from the top 2 cm of 58 giant box cores (Table 1, Fig. 2), and stored in a solution of ethanol and Rose Bengal to preserve and stain organic tissue (Lutze and Altenbach, 1991). After washing the sediment samples through a 63-µm sieve, rinsing with deionized water, and drying the remaining sand fraction at 50 °C, up to six single, ostracod valves per species and sample were picked for isotope analysis. The chosen ostracods were alive at sampling time or died shortly before, because all of them were stained red and did not bear any sign of calcite dissolution. Many of them contained chitinous appendices, were closed, or had left and right valves still attached together.

The valves were cleaned with deionized water, any chitinous appendages were removed, and, when possible, closed shells were opened and divided in two single valves. From the same species and the same sediment sample, all isotope measurements were done on either right or left valves in order to avoid measuring the same specimen twice. The maximum valve length (data available via http://www.pangaea.de) was measured to control size-dependent isotope fractionation as reported for other calcareous species, e.g. planktonic foraminifera

Table 1
Sediment and bottom water samples: location, sampling dates, salinity, temperature, and $\delta^{18}O$ of bottom water at sampling time

Station	Longitude (°E)	Latitude (°N)	Water depth (m)	Sampling date	Bottom salinity	Bottom temperature (°C)	$\delta^{18}O_{water}$ (‰ V-SMOW)
BP97-21	81.01	74.00	41	17–September–1997	32.60	−1.39	−1.73[a]
BP97-30	80.34	72.51	14	18–September–1997	12.63	4.81	−11.96[a]
BP97-42	81.67	73.90	32	20–September–1997	31.92	−1.18	−2.24[a]
BP97-43	82.81	73.71	31	20–September–1997	32.13	−1.11	−2.08[a]
BP97-47	73.75	72.58	18	22–September–1997	29.65	−0.47	−3.96[a]
BP97-48	73.15	72.96	29	22–September–1997	31.42	−1.37	−2.62[a]
BP97-49	72.89	73.21	29	23–September–1997	31.64	−1.36	−2.46[a]
BP97-50	72.95	73.61	28	23–September–1997	31.81	−0.07	−2.33[a]
BP97-52	72.66	74.00	30	24–September–1997	31.80	−1.35	−2.34[a]
BP99-01	74.10	74.46	27	24–August–1999	32.10	−1.58	−2.23
BP99-02	75.92	74.50	35	25–August–1999	32.20	−1.62	−2.28
BP99-03	80.01	74.00	37	26–August–1999	33.00	−1.64	−1.69
BP99-04	79.68	73.42	35	26–August–1999	32.50	−1.65	−1.71
BP99-08	79.99	72.93	21	27–August–1999	31.80	−1.21	−2.76
BP99-10	79.84	73.39	33	28–August–1999	32.76	−1.56	−1.61[a]
BP99-11	79.99	73.77	41	28–August–1999	32.10	−1.46	−2.00
BP99-12	79.48	73.76	25	28–August–1999	32.00	−1.60	−2.73
BP99-17	73.94	72.86	16	30–August–1999	30.40	−1.56	−3.77
BP99-19	74.19	72.19	14	31–August–1999	21.10	0.57	−8.07
BP99-20	74.73	72.51	16	1–September–1999	27.30	−1.01	−5.40
BP99-21	74.03	73.24	16	2–September–1999	30.15	−1.44	−3.59[a]
BP99-24	74.87	73.43	21	2–September–1999	29.70	−1.41	−4.23
BP99-25	74.00	74.00	26	3–September–1999	32.00	−1.54	−2.46
BP99-28	78.81	73.42	23	4–September–1999	29.50	−1.33	−4.17
BP99-29	78.51	73.09	16	4–September–1999	28.20	−1.18	−4.12
BP99-30	79.30	72.46	13	5–September–1999	16.50	3.95	−10.68
BP99-31	79.76	72.49	17	5–September–1999	29.70	−1.13	−3.81
BP99-32	79.95	73.13	27	6–September–1999	31.50	−1.55	−2.92
BP99-35	78.33	74.30	33	6–September–1999	33.00	−1.40	−1.49
BP99-37	74.33	74.30	30	7–September–1999	32.24	−1.54	−1.99[a]
BP99-38	75.61	74.25	31	7–September–1999	32.10	−1.52	−2.18
BP99-39	76.83	74.30	38	8–September–1999	32.73	−1.47	−1.62[a]
BP00-02	74.20	75.40	54	4–September–1900	33.30	−1.45	−0.87
BP00-05	81.01	75.84	55	6–September–2000	33.55	−1.38	−1.00[a]
BP00-07	81.14	74.66	43	7–September–2000	33.00	−1.37	−1.34
BP00-08	82.64	74.66	46	8–September–2000	33.29	−1.33	−1.20[a]
BP00-13	80.55	72.87	18	9–September–2000	30.20	−0.71	−3.00
BP00-15	81.60	72.05	11	10–September–2000	19.20	6.02	−8.47
BP00-26	77.96	75.71	73	15–September–2000	33.80	−1.42	−0.86
BP00-27	78.93	76.30	83	15–September–2000	34.20	−1.35	−0.56
BP00-28	83.88	76.66	55	16–September–2000	34.00	−1.37	−0.62
BP00-29	85.76	76.94	73	16–September–2000	34.20	−1.35	−0.71
BP00-30	83.04	75.99	57	17–September–2000	33.70		−0.89[a]
BP00-31	82.55	75.46	48	17–September–2000			
BP00-35	83.80	75.35	51	18–September–2000	33.50	−1.34	−0.94
BP00-36	81.96	76.96	71	19–September–2000	34.10	−1.35	−0.58
BP00-38	73.24	73.20	25	20–September–2000			
BP01-30	88.18	76.41	47	24–August–2001	34.13	−1.38	−0.56[a]
BP01-34	88.33	77.90	92	25–August–2001	34.28	−1.41	−0.45[a]
BP01-35	83.77	77.90	160	26–August–2001	34.70	−1.39	−0.13[a]

Table 1 (continued)

Station	Longitude (°E)	Latitude (°N)	Water depth (m)	Sampling date	Bottom salinity	Bottom temperature (°C)	$\delta^{18}O_{water}$ (‰ V-SMOW)
BP01-37	86.20	77.81	129	26 – August – 2001	34.46	− 1.39	− 0.31[a]
BP01-46	75.96	77.92	295	30 – August – 2001	34.88	− 0.68	0.01[a]
BP01-51	79.49	77.91	158	31 – August – 2001	34.52	− 1.20	− 0.27[a]
BP01-55	79.73	77.05	73	1 – September – 2001	34.03	− 1.39	− 0.64[a]
BP01-56	75.19	76.99	162	2 – September – 2001	34.80	− 0.86	− 0.05[a]
BP01-62	74.20	76.20	120	4 – September – 2001	34.30	− 1.34	− 0.43[a]
BP01-71	73.30	72.67	18	7 – September – 2001	31.39	− 0.42	− 2.64[a]
BP01-80	73.25	72.25	15	10 – September – 2001			

[a] Calculated from salinity (Eqs. (3)–(4)).

(Berger et al., 1978). The maximum shell lengths were different for different species and samples, but varied not more than 0.2 mm within a sample for the same species. No correlation between size and isotope data was detected. Since sizes of male carapaces can differ greatly from those of females (Horne et al., 2002) we assume that either the size difference between the sexes exceeds 0.2 mm and valves of only one sex were taken, or that there is no isotopic difference between male and female valves in the investigated species. The small size variations found here also make sure that only adult specimens were taken for isotope measurements, as adult carapaces are bigger than juveniles (De Deckker, 2002). Additionally, care was taken that the shell morphology, especially the calcified inner lamella, was well developed in all valves taken for isotope analyses.

Oxygen and stable carbon isotope compositions were measured on a Finnigan MAT 251 mass spectrometer with an automated Carbo-Kiel preparation line (Kiel Device I) at the Leibniz Laboratory of Kiel University. The $^{18}O/^{16}O$ and $^{13}C/^{12}C$ isotope ratios of carbonate samples are reported in the usual δ notation ($\delta^{18}O_{ostr}$ and $\delta^{13}C_{ostr}$, resp.; Rye and Sommer, 1980), versus the Peedee Belemnite (PDB) scale established via the NBS 20 (National Bureau of Standards) carbonate stable isotope standard. The analytical error is ± 0.07‰ for $\delta^{18}O$ and ± 0.04‰ for $\delta^{13}C$. Isotope data are available via http://www.pangaea.de.

2.2.2. Bottom water samples

The bottom water was sampled 1–2 cm above the sediment surface in subcores of a multicorer, which closes on both sides after penetrating the sediment, thereby preserving the original sediment surface with the water on top of it. The sampled water is assumed to be true bottom water (e.g. Mackensen et al., 2000). This assumption is corroborated by salinity measurements on 22 of these bottom water samples, which show that they were
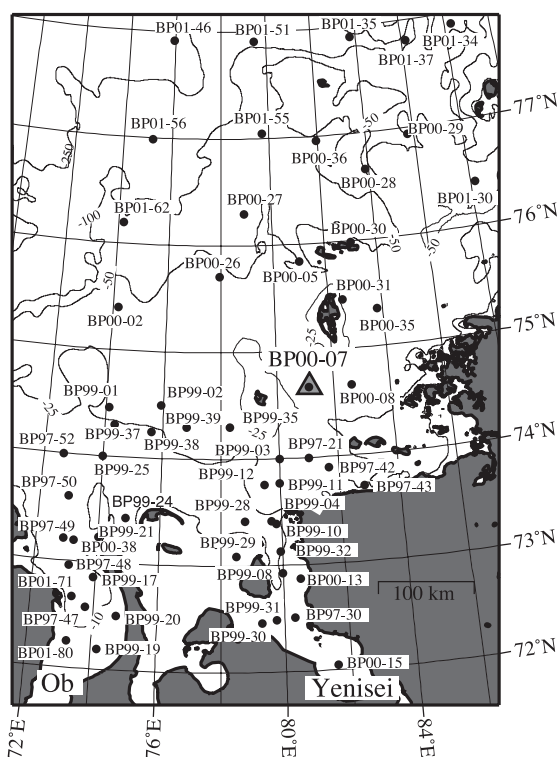

Fig. 2. Locations of sediment and water samples. Triangle marks location of gravity core BP00-07/5.

Table 2
AMS ^{14}C dates of core BP00-07/5

Depth[a] (cm)	Age (^{14}C years BP)	±	Reservoir correction	Age (cal. years BP)	1σ	Bivalve species	Sample number
35	1115	25	− 440	645	654 – 629	*P. arctica*	KIA 16376
155	3130	30	− 440	2845	2879 – 2806	*P. arctica*	KIA 16377
245	3965	30	− 440	3890	3934 – 3851	*P. arctica*	KIA 16378
365	5300	30	− 440	5600	5638 – 5584	*P. arctica*	KIA 16379
495	6510	35	− 440	6950	6996 – 6900	*P. arctica*	KIA 16380
625	7605	45	− 440	8000	8043 – 7954	*P. arctica*	KIA 16381

[a] Middle of 2-cm-thick sediment slices.

on average more saline by 0.4 than water sampled 1–2 m above the bottom in Niskin bottles of a rosette water sampler. If there were any possibility of exchange between the water entrapped in the multicorer and the ambient water during the haul of the multicorer aboard, salinity within the subcores would be less than in the Niskin bottles, which was not the case (Simstich, 2001).

The water samples were gently drawn free of air-bubbling into 100-ml crimp seal bottles, reduced by 1–2 ml to allow for thermal expansion, and poisoned by 0.2 ml saturated $HgCl_2$ solution (69 g $HgCl_2$ per litre at 20 °C). The bottles were sealed with a butyl rubber stop and kept cool in the dark. The oxygen isotope composition was measured at the Leibniz Laboratory applying the water–CO_2 equilibration method along with a Finnigan-MAT Delta E mass spectrometer (Erlenkeuser et al., 2003). External precision was ± 0.07‰ or better. All $\delta^{18}O_{water}$ values are reported on the Vienna-Standard Mean Ocean Water (V-SMOW) scale (Table 1). For salinity measurements, a hand-held conductivity meter of type LF320/330 from WTW, Weilheim, Germany with a measurement uncertainty of ± 0.1 was used.

2.2.3. Sampling the gravity core and age determination

Gravity core BP00-07/5 (632-cm core length) was collected during the expedition "SIRRO 2000" (Stein and Stepanets, 2001) from the shallow Kara Sea shelf (43-m water depth, 81.1°E, 74.7°N) north of Yenisei estuary (Fig. 2). Two-centimeter-thick sediment slices were taken in 5-cm steps along the core and washed through a 63-μm sieve. The remaining coarse fraction was rinsed with deionized water

and dried at 50 °C. Up to five (either left or right) single valves of *P. pseudopunctillata* were selected from every sample and analyzed for their stable isotope composition as described above. Like in the core tops (see above), no correlation was found between maximum shell length and isotope composition. Isotope data and shell lengths are available via http://www.pangaea.de.

Six radiocarbon ages (Table 2) were obtained from shells of the bivalve species *Portlandia arctica* by accelerator mass spectrometry (AMS) at the Leibniz Laboratory of Kiel University. Although the chosen bivalves were single-shelled and therefore not in situ, their preservation was good, indicating that they have not been transported for considerable distances. The AMS ^{14}C years are corrected for a reservoir effect of 440 years (Mangerud and Gulliksen, 1975) and converted to calendar years before present (cal. years BP)
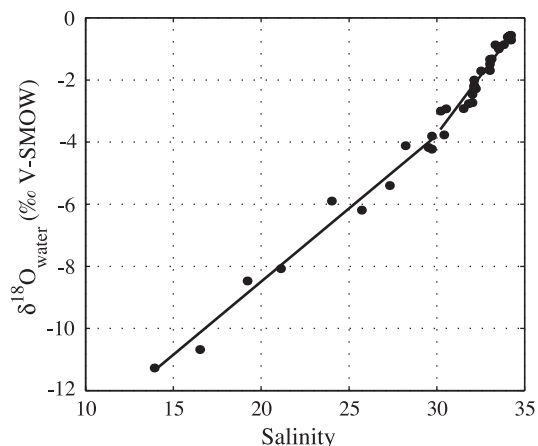

Fig. 3. Salinity and $\delta^{18}O_{water}$ values of bottom water samples. Regression lines for salinities above and below 30 are indicated.

by the programme CALIB rev.4.3 using the marine calibration data set (Stuiver and Reimer, 1993). Ages between the six dated fixpoints were estimated by linear interpolation and assuming a modern age for the sediment surface.

2.3. Calculations

Calculation of expected oxygen isotope values of calcite ($\delta^{18}O_{exp}$) precipitated in thermodynamic equilibrium with temperature (T) and $^{18}O/^{16}O$ ratio of ambient water ($\delta^{18}O_{water}$) follows the equation of

O'Neil et al. (1969); as cited by Shackleton, 1974; modified):

$$\delta^{18}O_{exp} = 21.9 - 3.16*(31.061 + T)^{0.5} + \delta_w \qquad (1)$$

This equation was chosen because it covers a temperature range down to 0 °C, which is closest to the temperature range of this study (-1.65 to approx. 0 °C). Applying the more recent paleotemperature equation of Kim and O'Neil (1997) would lead to equilibrium calcite values which are about 0.5‰ lower, thereby changing also the estimated biological frac-
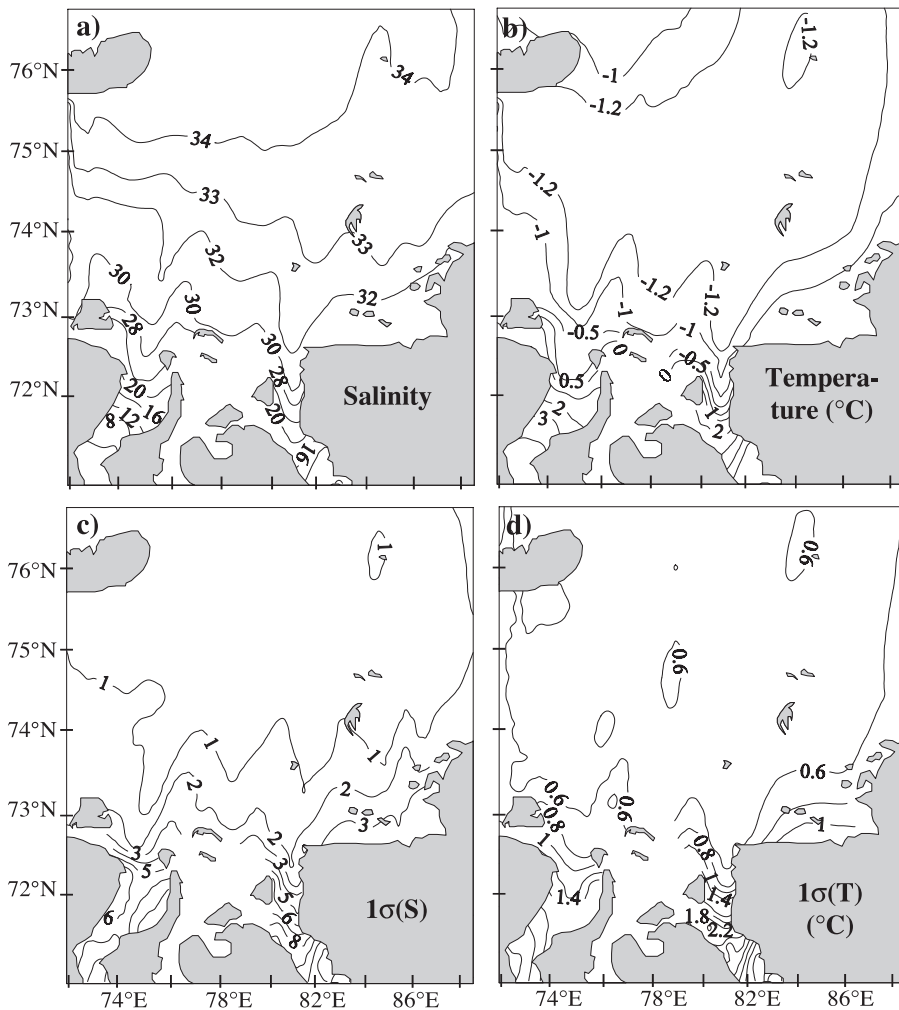

Fig. 4. Isohalines (a) and isotherms (b) of summer bottom water mean values (1929–2001). Isolines of standard deviation of salinity (c) and temperature (d).

tionation offsets by this value. Thus, the use of either of the two equations would yield different results on an absolute scale but would not affect the general scope of our study.

Conversion between $\delta^{18}O_{water}$ on the V-SMOW scale and δ_w follows (Hut, 1987):

$$\delta_w = 0.99973 * \delta^{18}O_{water,V-SMOW} - 0.27‰ \qquad (2)$$

Where $\delta^{18}O_{water}$ measurements are missing, we calculated them from bottom water salinity (S) following two relationships deduced from the bottom water samples of the Kara Sea (Fig. 3; Bauch et al., 2003):

Salinity$\leq 30 : \delta^{18}O_{water}$
$$= -17.9(\pm 0.59) + 0.47(\pm 0.02) \cdot S$$
$$(r^2 = 0.98, n = 11) \qquad (3)$$

Salinity $> 30 : \delta^{18}O_{water}$
$$= -26.5(\pm 1.53) + 0.76(\pm 0.05) \cdot S$$
$$(r^2 = 0.92, n = 24) \qquad (4)$$

The relationship between salinity and $\delta^{18}O_{water}$ in the Kara Sea is not linear between the endmembers river water and Atlantic Water, because sea ice formation contributes brine waters with high salinity but low $\delta^{18}O$ values to the bottom waters, thus skewing the salinity/$\delta^{18}O_{water}$ regression line in Fig. 3 towards the right (Bauch et al., 2003). For $S = 30$, both equations differ by 0.10‰

3. Results

3.1. Salinity and temperature distribution patterns

On average, summer bottom water salinity increases from zero in pure river water northwards to the shelf edge (Fig. 4a). Maximum salinity values above 34 are reached in the northwestern part of the investigation area, where water depths exceed 100 m. Average bottom water temperatures decrease from above 0 °C in the estuaries to values below −1.2 °C on the shelf (Fig. 4b). A reversal of this decreasing trend is obvious towards the northwest, in water deeper than 100 m, where temperatures increase to
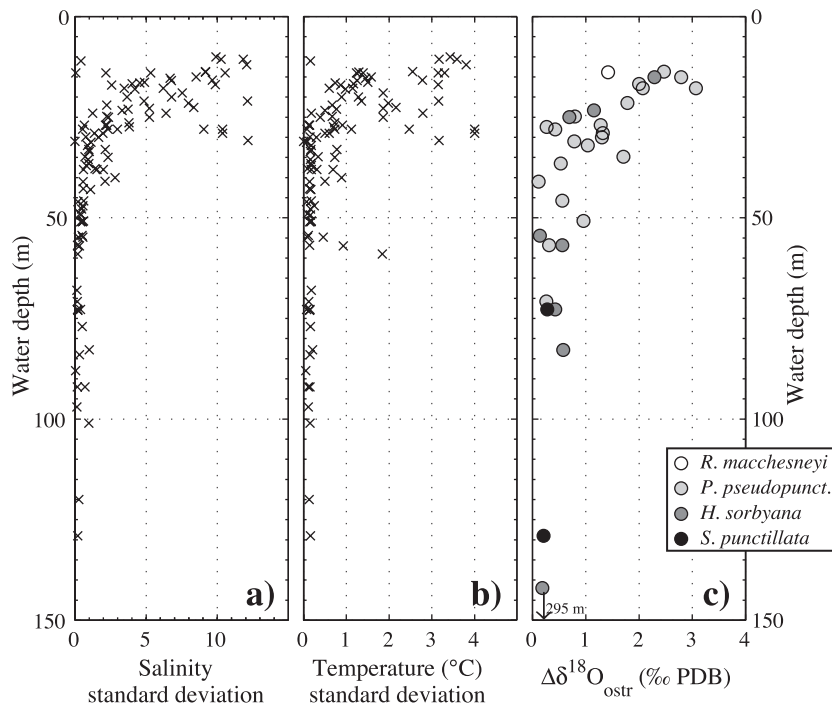

Fig. 5. Standard deviations of bottom salinity (a) and temperature (b) versus water depth. (c) Max.−min. $\delta^{18}O_{ostr}$ ranges obtained from sediment surface samples with five or more single-valve measurements per sample ($\Delta\delta^{18}O_{ostr}$) versus water depth.

values above -1 °C. The general south to north zonation of salinity and temperature is superimposed by a southward bending of the isohalines and isotherms in front of the estuaries of the rivers Ob and Yenisei.

The isolines of interannual variability (standard deviation; Fig. 4c, d) of salinity and temperature from the data sets closely resemble the patterns of the isohalines and isotherms. Even the southward bending in front of the estuaries is repeated. In general, the variabilities decrease with increasing distance from the estuaries, and with increasing water depth (Fig. 5a, b).

3.2. Distribution of stable isotopes in ostracod valves

Similar to salinity, the $\delta^{18}O$ and $\delta^{13}C$ values of the sampled ostracods, averaged for each station, increase northwards with distance to the river mouths and with water depth (Fig. 6). $\delta^{18}O$ values of *P. pseudopunctillata*, the most significant species in the area, range from <0‰ in the Ob estuary to >5‰ north of 75.5°N.

The minimum $\delta^{18}O$ value of -4.7‰ was determined for a sample in only 14-m water depth in the Ob estuary (BP01-80). $\delta^{13}C$ values range from <-6‰ to >-2‰ with extreme values around -13‰ in the Yenisei estuary (BP99-08). Similar to isohalines and isotherms, the $\delta^{18}O$ and $\delta^{13}C$ isolines bend southwards in front of the estuaries.

Most of the samples provided five or more single valves per species for isotope analyses. The max.–min. ranges of the obtained $\delta^{18}O$ and $\delta^{13}C$ values ($\Delta\delta$) were taken as measures for the isotopic variability of the individual samples. They reflect the rare extreme events in temperature and salinity more sensitively than standard deviations. Similar to the T/S variabilities in the hydrographic data sets, the $\Delta\delta$ ranges decrease with water depth (Fig. 5c) and distance to the river mouths (Fig. 7). Hence, samples with low variability ($\Delta\delta^{18}O \leq 0.5$‰) are not restricted to the outer shelf, but also can be found in troughs close to the estuaries. Conversely, moderately high $\Delta\delta^{18}O$ values up to 1.7‰ were determined for shallow areas 200 km north of the Ob
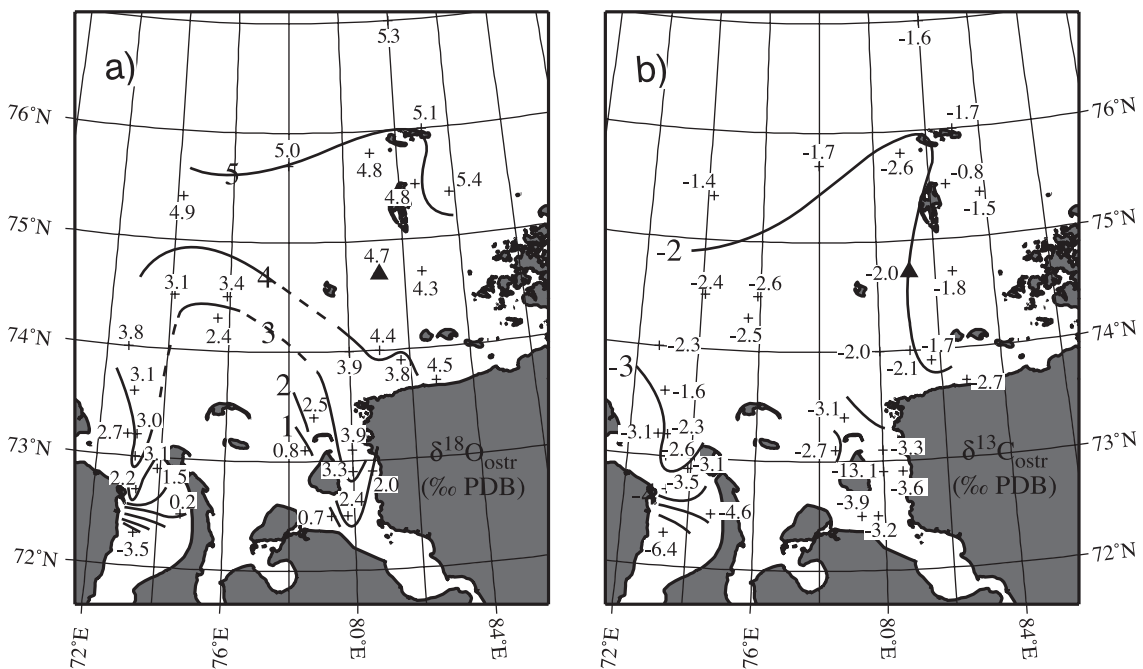

Fig. 6. Isolines of mean $\delta^{18}O$ (a) and $\delta^{13}C$ (b) of *P. pseudopunctillata* from core top samples with four or more measurements of single ostracod valves. Filled triangles mark location of gravity core BP00-07/5.

estuary. However, the highest variability with $\Delta\delta^{18}O$ values of approx. 3‰ is observed only in the mouth areas of the Ob and Yenisei estuaries (Fig. 7).

3.3. Downcore variations

Based on lithological core description and grain size estimates derived from smear-slide analyses, the sediments in core BP00-07/5 consist of silty clay to clayey silt with traces of bioturbation throughout the core (Stein et al., 2003). Many of valves of *P. pseudopunctillata* were found in the upper and lower core sections, but they were very rare to absent in the depth interval 220–490 cm (Fig. 8). Whenever possible, several single valves per sample were analyzed for their isotope composition. The analyses revealed considerable max.–min. $\delta^{18}O$ and $\delta^{13}C$ ranges ($\Delta\delta$) within the individual sediment samples. These $\Delta\delta$ ranges vary along the core from about 0.1‰ to 1.2‰ for $\delta^{18}O$ and from 0.2‰ to 1.7‰ for $\delta^{13}C$, around their mean values. The $\Delta\delta$ ranges are

Fig. 8. Stable isotope composition of single valves of *P. pseudopunctillata* from gravity core BP00-07/5. Thin horizontal lines connect isotope values of single valves from the same depth interval. Thick black lines connect mean values. Filled triangles mark core depths of AMS ^{14}C datings.

randomly distributed along the core, without significant differences between the upper and lower core sections.

Throughout the core, $\delta^{18}O$ and $\delta^{13}C$ are roughly positively correlated, i.e. depth intervals with low $\delta^{18}O$ values generally coincide with intervals of low $\delta^{13}C$, and vice versa (Fig. 8). The mean $\delta^{18}O$ values reveal a long-term trend from an average $\delta^{18}O$ of 4.8‰ in the lower core section (>400 cm) to 5.2‰ in the upper section. Correspondingly, $\delta^{13}C$ increases from $-2.2‰$ to $-1.6‰$

4. Discussion

4.1. Vital offsets

Comparison between hydrography and $\delta^{18}O$ in calcareous organisms requires corrections for biologically induced, species-specific vital offsets from the
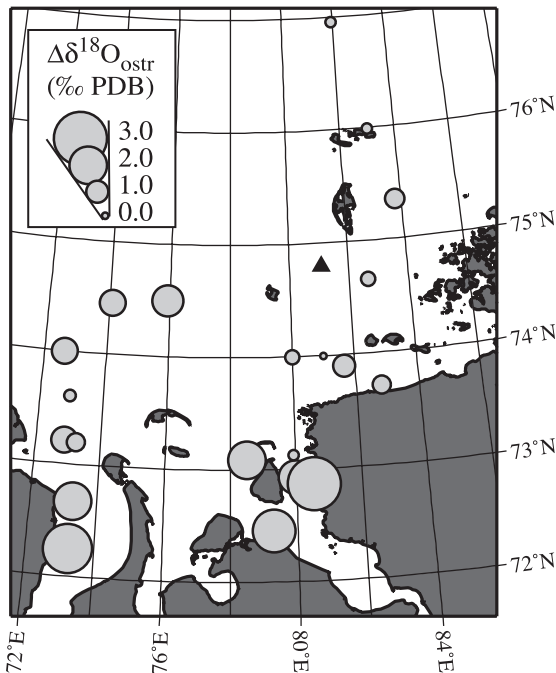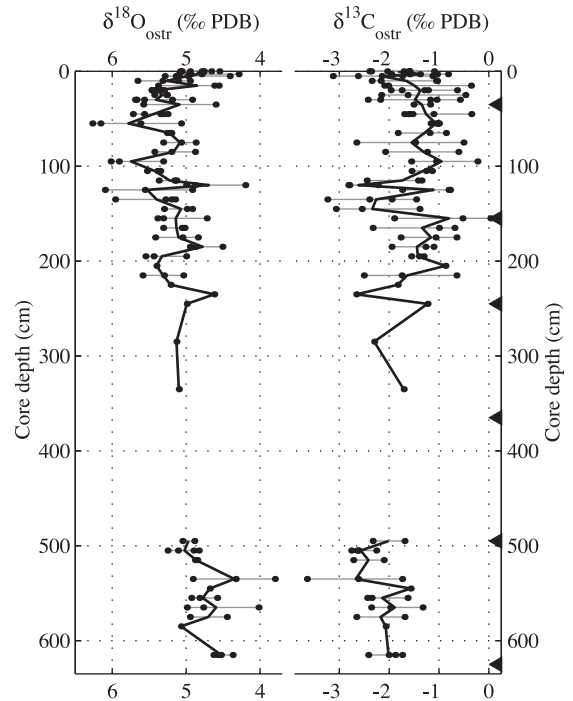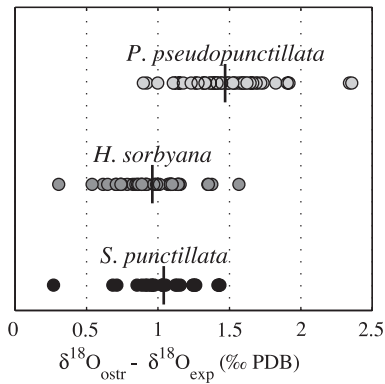

Fig. 7. Distribution of max.–min. $\delta^{18}O$ ranges of five or more single ostracod valves per sediment surface samples ($\Delta\delta^{18}O_{ostr}$). Filled triangle marks location of gravity core BP00-07/5.

Fig. 9. Vital offsets: differences ($\delta^{18}O_{ostr} - \delta^{18}O_{exp}$) between $\delta^{18}O_{ostr}$ values of single ostracod valves and corresponding $\delta^{18}O_{exp}$ values. Short vertical lines indicate averages.

equilibrium $\delta^{18}O_{exp}$ values defined in Eq. (1) (Urey et al., 1951). In a first, rough estimate Erlenkeuser and von Grafenstein (1999) deduced vital offsets for *P. pseudopunctillata* and *H. sorbyana* in the Laptev Sea to approximate 0‰ and − 0.5‰ respectively. They found that $\delta^{18}O$ deviations from equilibrium depend on water depth, because vital offsets in shallow water appear higher than in deeper water due to the higher hydrographic variability in shallow water. This is also the case in the Kara Sea, where salinity and temperature values in the data base are highly variable in water depths < 40 m, whereas they show only little variability in depths >40 m (Fig. 5a, b).

In order to reduce inaccuracies resulting from hydrographic variability in the estimates of vital offsets, we used only stations from >40 m water depth. The $\delta^{18}O_{exp}$ of each selected station was subtracted from the respective $\delta^{18}O_{ostr}$ values (Fig. 9). The average differences approximate the vital offsets to + 1.5‰ (standard deviation S.D. = ± 0.29‰, number of measurements $n = 55$) for *P. pseudopunctillata*, + 1.0‰ (S.D. = ± 0.24, $n = 42$) for *H. sorbyana*, and + 1.0‰ (S.D. = ± 0.26, $n = 24$) for *S. punctillata*. A vital offset for *R. macchesneyi* was not determined because this species only occurred in sediment samples from < 40-m water depth. We consider the present calculations of vital offsets for *P. pseudopunctillata* and *H. sorbyana* to be more significant than the previous estimates of Erlenkeuser and von Grafenstein (1999) because our results were based on

$\delta^{18}O_{water}$ and temperature data measured directly at the ostracod sampling sites and did not rely on extrapolated parameters.

4.2. Bottom hydrography and its influence on stable isotopes

4.2.1. Oxygen isotopes

Oxygen isotope compositions of biogenic calcite mirror mainly salinity (via $\delta^{18}O_{water}$) and temperature (see Eqs. (1)–(4)). To compare ostracod isotope signals with hydrography, the equilibrium $\delta^{18}O_{exp}$ values expected for calcite precipitation in bottom water were calculated for every grid point of the hydrographic data base for mean summer bottom salinity and temperature (Fig. 10). The vital offset of *P. pseudopunctillata* was added to the results to adjust them to the measured $\delta^{18}O_{ostr}$ values. The general correspondence between the adjusted $\delta^{18}O_{exp}$ pattern (Fig. 10) and the measured $\delta^{18}O_{ostr}$ pattern of *P. pseudopunctillata* (Fig. 6a) shows that the oxygen isotope composition of the ostracod valves truly records the mean bottom water hydrog-
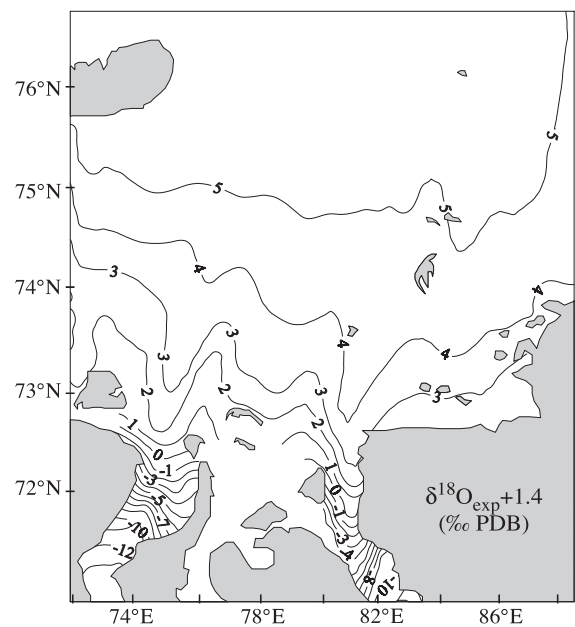

Fig. 10. Isolines of calculated benthic $\delta^{18}O$ expected for calcite precipitation in isotopic equilibrium with the water at summer temperature and bottom $\delta^{18}O_{water}$ (Eqs. (1)–(4)). 1.4‰ is added to account for vital offset of *P. pseudopunctillata*.

raphy and can be used as a reliable tool for the reconstruction of past conditions in shallow marine environments. Differences of $1–4‰$ between $\delta^{18}O_{exp}$ and $\delta^{18}O_{ostr}$ in the estuary mouths indicate the strong hydrographic variability in the frontal zones (see discussion below).

The characteristics of the Kara Sea Bottom Water are considerably determined by the admixture of Atlantic Water, river water, and brine water (Bauch et al., 2003). The northward increase of salinity and the slight temperature increase in the northwestern Kara Sea (Fig. 4a, b) illustrate the entrainment of traces of the originally highly saline (>34.9) and relatively warm (>0 °C) waters of Atlantic origin into the Kara Sea from the Arctic basin and the Barents Sea (Aagaard et al., 1985). Albeit observable in salinity and temperature trends, this water mass is neither distinguishable in the oxygen isotope signatures of the ostracods (Fig. 6a) nor in the $\delta^{18}O_{exp}$ field (Fig. 10). The reason is that the presently observed temperature increase from -1.2 to -1.0 °C in the northwestern investigation area affects the oxygen isotope composition of calcite by only $-0.06‰$ (Eq. (1)). This drop is much smaller than the contemporaneous salinity effect of $+0.49‰$ expected from an increase of the salt content by $S=1$ (Eqs. (1)–(4)).

Based on simple mass balance calculations, approximately 10% of the Kara Sea Bottom Water comes from brine release during sea ice formation in fall and winter in a reoccurring flaw polynya on the shelf (Bauch et al., 2003). These very dense and cold brine waters mix with the prevailing bottom water but the mass of brine water is not enough to be distinguishable in the $\delta^{18}O$ distributions of ostracods and the equilibrium $\delta^{18}O_{exp}$.

The imprint of river water, however, is clearly visible in the isotope ratios. The maximum peak of river discharge floods the shallow shelf within a few weeks in early summer and induces a very strong seasonal pycnocline of up to $1–2$ °C and $5–8$ salinity units per 10 cm in $5–12$-m water depth (Shmelkov et al., 2002), which is an enormous barrier to vertical mixing. However, the remarkably low $\delta^{18}O_{ostr}$ values at the sea floor of the southern Kara Sea (Fig. 6a) indicate that significant amounts of river water are mixed down to the bottom, despite the strong density gradient in the summer pycnocline. This finding is corroborated by subannual cycles of bottom water freshening, found in stable isotope profiles from mussel shells collected in 30-m water depth north of the Ob and Yenisei mouths (Simstich et al., 2003).

The southward bending isotherms, isohalines, and $\delta^{18}O_{ostr}$ isolines in front of the estuaries (Figs. 4 and 6) indicate a southward penetration of cold, saline bottom waters, a phenomenon also visible in dynamic shelf models (Harms and Karcher, 1999). Flow meter studies in the neighboring Laptev Sea have shown that cold, saline marine waters flow onto the shelf to water depths as shallow as 50 m in counter currents which are driven by wind and river run-off (Dmitrenko et al., 2001). The preferred routes for counter currents are former Pleistocene river channels, which are also found in the Kara Sea as submarine continuations of the Ob and Yenisei river channels (Stein et al., 2002; Dittmers et al., 2003).

4.2.2. Stable carbon isotopes

The different sources contributing to the bottom water are also reflected in the carbon isotope ratios of *P. pseudopunctillata* (Fig. 6b). The carbon isotope composition of ostracod valves is governed by $\delta^{13}C$ of dissolved inorganic carbon (DIC) in the water, because DIC is the main carbon source for valve calcite (Simkiss and Wilbur, 1989). DIC is ^{13}C-enriched in marine waters ($\delta^{13}C_{DIC}$: -3 to $0‰$) and ^{13}C-depleted in river waters of Ob and Yenisei ($\delta^{13}C_{DIC}$: approx. $-7.6‰$) (Erlenkeuser et al., 1999; Kodina et al., 1999). Taking up carbon with different portions of marine and river DIC, the resulting $\delta^{13}C$ values in ostracod valves are lower near the estuaries than in the deeper water further to the north (Fig. 6b).

A second carbon source for valve secretion is animal-internal, metabolically derived CO_2. Its isotope composition is closely connected to the $\delta^{13}C$ signal of the consumed food, which is mainly particulate organic carbon (POC) taken up from the sediment surface (Simkiss and Wilbur, 1989; McConnaughey et al., 1997). $\delta^{13}C$ of POC in surface sediments and water samples of the Kara Sea is lower in the estuaries due to river influence ($-28‰$ to $-26‰$) than in the more marine sediments and waters of the outer shelf ($-25‰$ to $-24‰$; Kodina and Peresypkin, 2002). Thus, feeding on POC from different sources and with different $\delta^{13}C$ signature will add to the northward increase of the stable carbon isotope ratios in ostracod valves (Fig. 6b).

4.3. Modern variability in the bottom water

After the last molting, ostracods can live up to 3 years in the same carapace. Therefore, populations are composed of multiple overlapping generations that attained their last molting stage at different times, as was reported for some freshwater species (Kesling, 1961; Xia et al., 1997; Horne et al., 2002). Based on that, the isotopic composition of a single (stained) ostracod valve from a sediment surface sample could represent the hydrographic conditions at a certain, but unknown time in any summer of the last 3 years. This assumption may help to explain the max.−min. ranges ($\Delta\delta$; Figs. 5c and 7) in the isotope data of those samples which provided several single shells per sample for analyses. The $\Delta\delta$ values strongly suggest that not all specimens within these samples—although living—secreted their valves under the same hydrographic conditions. For example, the $\Delta\delta^{18}O$ range of 0.69‰ in *H. sorbyana* at site BP99-12 (79.5°E, 73.8°N, 25 m) can be explained by a salinity difference of approx. 0.9 or by a temperature change of approx. 2 °C (Eqs. (1)−(4)) between secretion of the two valves with the extreme $\delta^{18}O$ values. The required temperature change of 2 °C is not very likely for that location, where temperature standard deviations of only ± 0.6 °C are observed (Fig. 4d). Salinity, however, varies by ± 1.5 (Fig. 4c) and therefore easily outweighs the temperature influence. Usually temperature varies with salinity, and actually both changes (e.g. T: ± 0.6 °C and S: ± 0.7) contributed to the observed $\Delta\delta^{18}O$.

Tidal- and wind-driven *T/S* changes certainly do not induce enough change in the bottom water properties to affect the $\delta^{18}O$ signals of the ostracods significantly. The observed $\Delta\delta^{18}O$ likely reflects longer lasting *T/S* changes at the bottom. The most profound hydrographic influence on the Kara Sea shelf is the huge amount of river water released every spring and summer by the rivers Ob and Yenisei. These river waters have a relatively high temperature above 10 °C, zero salinity, and very low $\delta^{18}O_{water}$ of − 16‰ to − 18‰ (Brezgunov et al., 1983; Bauch et al., 2003). Thus, the contribution of even small amounts of river water induces more changes in the bottom water properties and affects the ostracod oxygen isotope signals more than equal amounts of Atlantic Water and brine water can do (see discussion above).

The extreme seasonal and interannual variability of the river water supply combined with the behaviour of individual ostracods to molt at different times evidently result in isotope signals which differ from valve to valve within the same sediment sample. Thus, stable isotope analyses on several single ostracod valves per sample provide a tool for paleoceanographic reconstructions of the *T/S* variability at the bottom of shallow Eurasian shelf seas and in the vicinity of river mouths finally addressing the extent of the riverine influence on the shelf hydrography. On the other hand, a prerequisite for paleoceanographic applications is that a fairly large number of fossil ostracods have to be analyzed from each individual sediment sample to eliminate seasonal and interannual noise.

4.4. Holocene variability in the bottom water

Recent research in the Kara Sea (Polyak et al., 2000, 2002, 2003; Lubinski et al., 2001, Stein et al., 2003) has shown that the most profound hydrographic changes during the Holocene resulted from global sea level rise due to the melting of the glacial ice sheets. Isotopically, the decay of the residual ice masses since 8000 BP made the $\delta^{18}O_{water}$ change by approx. − 0.18‰ (Fairbanks, 1989). After correction for these $\delta^{18}O_{water}$ changes, the $\delta^{18}O_{ostr}$ record of core BP00-07/5 reveals an average of 4.6‰ in the interval before 7000 cal. years BP and 5.2‰ after 5000 cal. years BP (Fig. 11). This $\delta^{18}O$ shift indicates a diminishing influence of fluvial water at the core location and illustrates the southward retreat of the river mouths across the shelf to their modern estuaries. The difference of 0.6‰ $\delta^{18}O$ between the upper and lower core sections suggests that salinity in the bottom water increased by roughly 1 (Eqs. (1)−(4)). Under present conditions, a change of this magnitude implies a southward retreat of the river mouth by approx. 100 km from the coring site.

In core samples providing several ostracod valves for analyses, the max.−min. isotope ranges were expected to be higher prior to 7000 cal. years BP than after 5000 cal. years BP because the vicinity to the paleo-river mouths suggests a higher *T/S* variability, as is the case for recent sediment surface samples near the estuaries (Fig. 7). However, there

is no evidence a systematic change between the isotope ranges in the lower and upper core sections (Fig. 8). This finding indicates that, simultaneously with sea level rise and retreating river mouths, other factors like bathymetric changes and the bottom water flow influenced the hydrography at the core location in such a way that the hydrographic variability did not change substantially in the course of the Holocene.

Today, low max.−min. isotope ranges can be found in river-proximal samples, when they come from submarine paleo-river channels (Fig. 7). Seismic profiling has shown that site BP00-07/5 was originally situated in such a submarine channel of paleo-Yenisei which filled up with sediment during the Holocene and became a flat plane (Fig. 12b; Dittmers and Stein, 2001). Additionally, the location may have been located deeper in the time interval before 7000 cal. years BP due to the incomplete isostatic uplift following the decay of the Late Weichselian ice sheet over the Barents and Kara sea shelves (Forman et al., 1995). The isostatic uplift
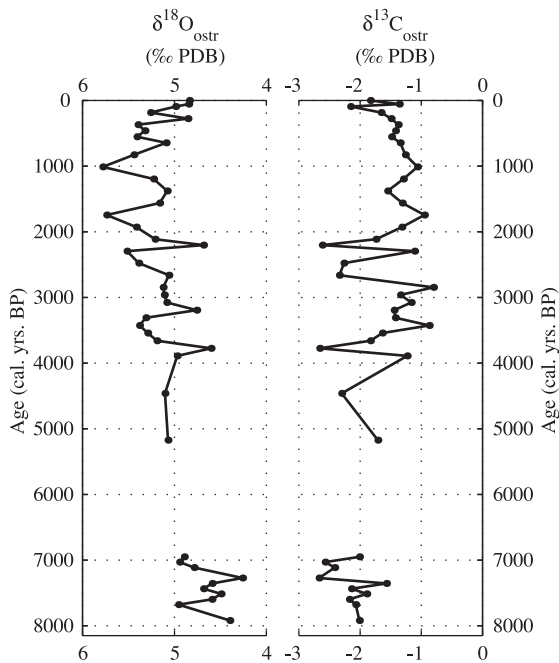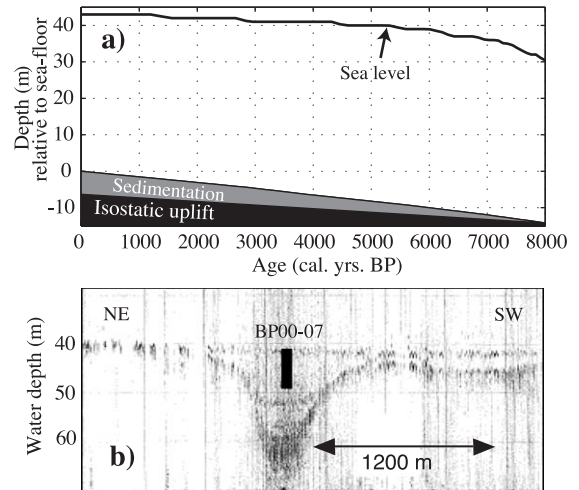
Fig. 12. (a) Holocene water depth at site BP00-07 derived from global sea level change (Fairbanks, 1989), isostatic uplift (Aller and Uhl, 1931; cited in Forman et al., 1995), and sediment filling of the submarine channel of paleo-Yenisei as shown in the sediment echograph profile (b; Dittmers and Stein, 2001).

is assumed to amount up to 5 m since 5000 BP at the Izvestia Tsik Islands (Aller and Uhl, 1931; cited in the work of Forman et al., 1995) approx. 150 km north of the coring site at 83°E, 76°N. These Islands are located in between the core location and the edge of the former ice-sheet. (Svendsen et al., 2004). Therefore, linear extrapolation of 5 m uplift at Izvestia Tsik Islands to the core location and backwards to 8000 BP reveals an maximum isostatic depression of 8 m.

Resulting from the combined effect of global sea level rise, rapid sedimentation and isostatic uplift, the distance of the river mouth to the core location increased, but the water depth remained approximately the same since 8000 cal. years BP (Fig. 12). Already prior to 7000 cal. years BP the influence of the variability in river water supply on the properties of the bottom water was balanced by the advection of cold saline water along the paleo-channel. Sediment filling of this channel during the Holocene should initially permit a higher hydrographic variability, but the simultaneous retreat of the river mouth counteracted the expected development and resulted in a diminishing influence of river

Fig. 11. Mean $\delta^{18}O$ and $\delta^{13}C$ values of *P. pseudopunctillata* in core BP00-07/5 versus calendar age. $\delta^{18}O$ values are corrected for the global ice effect (Fairbanks, 1989).

run-off and its extreme seasonal and interannual variability at the coring site.

5. Conclusions

The distribution pattern of $\delta^{18}O$ values of living benthic ostracods from the Kara Sea corresponds to calculated inorganic $\delta^{18}O$ as expected from long-term bottom water salinity and temperature means and corrected for species specific vital offsets. Similarly, the isotope ranges (max.−min.) obtained from measuring several single ostracod valves per sediment surface sample mirror the hydrographic variability in the bottom water. Thus, repeated $\delta^{18}O$ measurements on single ostracod valves provide a useful tool for the reconstruction of past hydrographic changes in Eurasian shelf seas. Low $\delta^{18}O$ and $\delta^{13}C$ values with high in-sample variability (max.−min. isotope ranges) indicate a strong influence of riverine freshwater on the bottom water hydrography near river mouths. Higher isotope values with lower in-sample variability indicate a higher contribution of Atlantic-derived water to the bottom water on the deeper shelf and in submarine paleo-river channels.

Resulting from the combined effects of global sea level rise, rapid sedimentation and isostatic uplift, the paleo-water depth at the coring site in a submarine paleo-river channel north of Yenisei remained approximately the same since 8000 cal. years BP, while the distance of the coring site to the river mouth increased during the Holocene. Both facts are reflected in the observation that the isotopic variability (max.−min. ranges) obtained from repeated single-valve measurements in individual samples along the core did not change systematically through time, but that the mean $\delta^{18}O$ values are lower before 7000 cal. years BP than in the Late Holocene. The low $\delta^{18}O$ level indicates a higher contribution of river water before 7000 cal. years BP than later when the global sea level rise induced a southward retreat of the river mouth from the coring site. Prior to 7000 cal. years BP the expected higher, river-proximal hydrographic variability at the coring site was probably buffered by a relatively stable advection of cold, saline water from the outer shelf along a submarine channel of the paleo-Yenisei. Rapid sedimentation filled the paleo-channel and isostatic uplift elevated the coring site during the Holocene,

but the hydrographic variability did not increase because the influence of the highly variable river water discharge on the bottom hydrography diminished with the southward retreat of the river mouth.

References

Aagaard, K., Swift, J.H., Carmack, E.C., 1985. Thermohaline circulation in the Arctic Mediterranean seas. Journal of Geophysical Research 90 (C3), 4833–4846.

Aller, G.D., Uhl, G.F., 1931. The Izvestia Islands. Komintern and Shkola FZU im KIM'a. Leningrad 80 pp.

Alley, R.B., 1995. Resolved: the Arctic controls global climate change. In: Smith Jr., W.O., Grebmeier, J.M. (Eds.), Arctic Oceanography: Marginal ice zones and continental shelves. Coastal and Estuarine Studies. American Geophysical Union, Washington, DC, pp. 263–283.

Bauch, D., Erlenkeuser, H., Stanovoy, V., Simstich, J., Spielhagen, R., 2003. Freshwater distribution and brine waters in the southern Kara Sea in summer 1999 as depicted by $\delta^{18}O$ results. In: Stein, R., Fahl, K., Fütterer, D.K., Galimov, E.M., Stepanets, O.V. (Eds.), Siberian River Run-off in the Kara Sea: Characterisation, Quantification, Variability and Environmental Significance. Proceedings in Marine Sciences, vol. 6. Elsevier, Amsterdam, pp. 73–90.

Benson, R.H., 1961. Ecology of ostracode assemblages. In: Moore, R.C., Pitrat, C.W. (Eds.), Treatise on Invertebrate Paleontology. Geological Society of America, pp. Q56–Q63.

Benson, R.H., Delgrosso, R.M., Steineck, P.L., 1983. Ostracode distribution and biofacies, Newfoundland continental slope and rise. Micropaleontology 29 (4), 430–453.

Berger, W.H., Killingley, J.S., Vincent, E., 1978. Stable isotopes in deep-sea carbonates: box core ERDC-92, west equatorial Pacific. Oceanologica Acta 1, 203–216.

Brezgunov, V.S., Debol'skii, V., Nechaev, V.V., Ferronskii, V.I., Yakimova, T.V., 1983. Characteristics of the formation of the oxygen isotope composition and salinity upon mixing of sea and river waters in the Barents and Kara Seas. Water Resources, Translation of Vodnye Resursy 9 (4), 335–344.

Davis, J.C., 1986. Statistics and Data Analysis in Geology, 2nd ed. Wiley, New York. 646 pp.

De Deckker, P., 2002. Ostracod paleoecology. In: Holmes, J.A., Chivas, A.R. (Eds.), The Ostracoda: Applications in Quaternary Research. American Geophysical Union Monograph Series, pp. 121–134.

Dittmers, K., Stein, R., 2001. 3.5 kHz and ELAC sediment echograph profiling. Berichte zur Polar-und Meeresforschung—Reports on Polar and Marine Research 393, 84–88.

Dittmers, K., Niessen, F., Stein, R., 2003. Holocene sediment budget and sedimentary history for the Ob and Yenisei estuaries. In: Stein, R., Fahl, K., Fütterer, D.K., Galimov, E.M., Stepanets, O.V. (Eds.), Siberian River Run-off in the Kara Sea: Characterisation, Quantification, Variability and Environmental Significance. Proceedings in Marine Sciences, vol. 6. Elsevier, Amsterdam, pp. 457–470.

Dmitrenko, I., Golovin, P., Gribanov, V., Kassens, H., Hölemann, J., 1998. Influence of the summer river runoff on ice formation in the Kara and Laptev Seas. In: Shen. (Ed.), Ice in Surface Waters. Balkema, Rotterdam, pp. 251–257.

Dmitrenko, I.A., Hölemann, J.A., Kirillov, S.A., Wegner, C., Gribanov, V.A., Berezovskaya, S.L., Kassens, H., 2001. Thermal regime of the Laptev Sea bottom layer and affecting processes. Kriosfera Zemli 3, 40–55 (In Russian).

Erlenkeuser, H., von Grafenstein, U., 1999. Stable oxygen isotope ratios in benthic carbonate shells of ostracoda, foraminifera, and bivalvia from surface sediments of the Laptev Sea, summer 1993 and 1994. In: Kassens, H., Bauch, H.A., Dmitrenko, I., Eicken, H., Hubberten, H.-W., Melles, M., Thiede, J., Timokhov, L. (Eds.), Land–ocean systems in the Siberian Arctic: Dynamics and history. Springer-Verlag, Berlin, pp. 503–514.

Erlenkeuser, H., Spielhagen, R.F., Taldenkova, E., 1999. Stable isotopes in modern water and bivalve samples from the southern Kara Sea. Berichte zur Polarforschung—Reports on Polar Research 300, 80–90.

Erlenkeuser, H., Cordt, H.H., Simstich, J., Bauch, D., Spielhagen, R., 2003. DIC stable carbon isotope pattern in the surface waters of the southern Kara Sea, Sep. 2000. In: Stein, R., Fahl, K., Fütterer, D.K., Galimov, E.M., Stepanets, O.V. (Eds.), Siberian River Run-off in the Kara Sea: Characterisation, Quantification, Variability and Environmental Significance. Proceedings in Marine Sciences, vol. 6. Elsevier, Amsterdam, pp. 91–110.

Fairbanks, R.G., 1989. A 17,000-year glacio-eustatic sea level record: influence of glacial melting rates on the Younger Dryas event and deep ocean circulation. Nature 342, 637–642.

Forman, S.L., Lubinski, D., Miller, G.H., Snyder, J., Matishov, G.,

Korsun, S., Myslivets, V., 1995. Postglacial emergence and distribution of late Weichselian ice-sheet loads in the northern Barents and Kara seas, Russia. Geology 23 (2), 113–116.

Harms, I.H., Karcher, M.J., 1999. Modeling the seasonal variability of hydrography and circulation in the Kara Sea. Journal of Geophysical Research 104 (C6), 13,431–13,448.

Horne, D.J., Cohen, A., Martens, K., 2002. Taxonomy, morphology and biology of Quaternary and living ostracoda. In: Holmes, J.A., Chivas, A.R. (Eds.), The Ostracoda: Applications in Quaternary Research. American Geophysical Union Monograph Series, pp. 5–36.

Hut, G., 1987. Consultants' group meeting on stable isotope reference samples for geochemical and hydrological investigations, 16.-18.9.1985. Report to the Director General, International Atomic Energy Agency, Vienna.

Kesling, R.V., 1961. Ontogeny of ostracoda. In: Moore, R.C., Pitrat, C.W. (Eds.), Treatise on Invertebrate Paleontology. Geol. Soc. Am., Q19–Q20.

Kim, S.-T., O'Neil, J.R., 1997. Equilibrium and nonequilibrium oxygen isotope effects in synthetic carbonates. Geochimica et Cosmochimica Acta 61 (16), 3461–3475.

Kodina, L.A., Peresypkin, V.I., 2002. Stable carbon isotope ($\delta^{13}C_{org}$) ratio and lignin-derived phenol distribution in surface sediments of the inner Kara Sea. Berichte zur Polar-und Meeresforschung—Reports on Polar and Marine Research 419, 134–142.

Kodina, L.A., Bogacheva, M.P., Vlasova, L.N., Meschanov, S.L., Ljutsarev, S.V., 1999. Isotope geochemistry of particulate organic carbon in the Yenisei estuary: sources and regularities of distribution. In: Matthiessen, J., Stepanets, O., Stein, R., Fütterer, D.K., Galimov, E.M. (Eds.), The Kara Sea Expedition of RV "Akademik Boris Petrov" 1997: First results of a joint Russian–German pilot study. Berichte zur Polarforschung—Reports on Polar Research. Alfred Wegener Institute for Polar and Marine Research, Bremerhaven, pp. 91–101.

Lubinski, D.J., Polyak, L., Forman, S.L., 2001. Freshwater and Atlantic water inflows to the deep northern Barents and Kara seas since ca 13 ^{14}C ka: foraminifera and stable isotopes. Quaternary Science Reviews 20 (18), 1851–1879.

Lutze, G.F., Altenbach, A., 1991. Technik und Signifikanz der Lebendfärbung benthischer Foraminiferen mit Bengalrot. Geologisches Jahrbuch, A 128, 251–265.

Mackensen, A., Schumacher, S., Radke, J., Schmidt, D.N., 2000. Microhabitat preferences and stable carbon isotopes of endobenthic foraminifera: clue to quantitative reconstruction of oceanic new production? Marine Micropaleontology 40 (3), 233–258.

Mangerud, J., Gulliksen, S., 1975. Apparent radiocarbon ages of recent marine shells from Norway, Spitsbergen, and Arctic Canada. Quaternary Research 5, 273–296.

Matthiessen, J., Stepanets, O. (Eds.), 1998. Scientific Cruise Report of the Kara Sea Expedition of RV "Akademik Boris Petrov" in 1997. Berichte zur Polarforschung—Reports on Polar Research, 266. 102 pp.

McConnaughey, T.A., Burdett, J., Whelan, J.F., Paull, C.K., 1997. Carbon isotopes in biological carbonates: respiration

and photosynthesis. Geochimica et Cosmochimica Acta 61 (3), 611–622.

McCorkle, D.C., Corliss, B.H., Farnham, C.A., 1997. Vertical distributions and stable isotopic compositions of live (stained) benthic foraminifera from the North Carolina and California continental margin. Deep-Sea Research. Part 1. Oceanographic Research Papers 44 (6), 983–1024.

Millero, F.J., 1993. What is PSU? Oceanography 6 (3), 67.

Moritz, R.E., Bitz, C.M., Steig, E.J., 2002. Dynamics of recent climate change in the Arctic. Science 297, 1497–1503.

Olli, K., Riser, C.W., Wassmann, P., Ratkova, T., Arashkevich, E., Pasternak, A., 2002. Seasonal variation in vertical flux of biogenic matter in the marginal ice zone and the central Barents Sea. Journal of Marine Systems 38 (1–2), 189–204.

O'Neil, J.R., Clayton, R.N., Mayeda, T.K., 1969. Oxygen isotope fractionation in divalent metal carbonates. The Journal of Chemical Physics 51 (12), 5547–5558.

Pavlov, V.K., Pfirman, S.L., 1995. Hydrographic structure and variability of the Kara Sea: implications for pollutant distribution. Deep-Sea Research. Part 2. Topical Studies in Oceanography 42 (6), 1369–1390.

Peterson, B.J., Holmes, R.M., McClelland, J.W., Vörösmarty, C.J., Lammers, R.B., Shiklomanov, A.I., Shiklomanov, I.A., Rahmstorf, S., 2002. Increasing river discharge to the Arctic Ocean. Science 298, 2171–2173.

Peypouquet, J.P., Carbonel, P., Ducasse, O., Tolderer-Farmer, M., Lete, C., 1988. Environmentally cued polymorphism of ostracods. In: Hanai, T., Ikeya, T., Ishizaki, K. (Eds.), Evolutionary Biology of Ostracoda. Its Fundamentals and Applications. Elsevier, Amsterdam, pp. 1003–1019.

Polyak, L., Levitan, M., Gataullin, V., Khusid, T., Mikhailov, V., Mukhina, V., 2000. The impact of glaciation, river-discharge and sea-level change on Late Quaternary environments in the southwestern Kara Sea. International Journal of Earth Sciences 89 (3), 550–562.

Polyak, L., Levitan, M., Khusid, T., Merklin, L., Mukhina, V., 2002. Variations in the influence of riverine discharge on the Kara Sea during the last deglaciation and the Holocene. Global and Planetary Change 32, 291–309.

Polyak, L., Stanovoy, V., Lubinski, D.J., 2003. Stable isotopes in benthic foraminiferal calcite from a river-influenced arctic marine environment, Kara and Pechora seas. Paleoceanography 18 (1), 1003 (doi:10.1029/2001PA000752).

Polyakov, I.V., Johnson, M.A., 2000. Arctic decadal and interdecadal variability. Geophysical Research Letters 27 (24), 4097–4100.

Proshutinsky, A.Y., Polyakov, I.V., Johnson, M.A., 1999. Climate states and variability of Arctic ice and water dynamics during 1946–1997. Polar Research 18 (2), 135–142.

Rye, D.M., Sommer, M.A., 1980. Reconstructing paleotemperature and paleosalinity regimes with oxygen isotopes. In: Rhoads, D.C., Lutz, R.A. (Eds.), Skeletal Growth of Aquatic Organisms. Topics in Geobiology. Plenum, New York, pp. 169–202.

Sanders, T.M., Garvine, R.W., 2001. Fresh water delivery to the continental shelf and subsequent mixing: an observational study. Journal of Geophysical Research 106 (C11),

27087–27101.

Scourse, J.D., Austin, W.E.N., 2002. Quaternary shelf sea palaeoceanography: recent developments in Europe. Marine Geology 191 (3–4), 87–94.

Semiletov, I.P., Savelieva, N.I., Weller, G.E., Pipko, I.I., Pugach, S.P., Gukov, A.Y., Vasilevskaya, L.N., 2000. The dispersion of Siberian river flows into coastal waters: meteorological, hydrological and hydrochemical aspects. In: Lewis, E.L. (Ed.), The Freshwater Budget of the Arctic OceanNATO Sciences Series. Kluwer Academic Publishing, Dordrecht, pp. 323–366.

Shackleton, N.J., 1974. Attainment of isotopic equilibrium between ocean water and the benthonic foraminifera genus *Uvigerina*: isotopic changes in the ocean during the last Glacial. Colloques Internationaux du CNRS 219, 203–209.

Shmelkov, B., Latko, A., Stanovoy, V., 2002. Hydrological conditions in the Kara Sea during summer cruise 2001. Berichte zur Polar-und Meeresforschung—Reports on Polar and Marine Research 419, 6–12.

Simkiss, K., Wilbur, K.M., 1989. Biomineralization—Cell Biology and Mineral Deposition. Academic Press, San Diego. 337 pp.

Simstich, J., 2001. Is water from the rosette sampler a suitable proxy for bottom water? Comparison of salinity in rosette and multicorer. Berichte zur Polar-und Meeresforschung—Reports on Polar and Marine Research 393, 18–20.

Simstich, J., Stanovoy, V., Novikhin, A., Erlenkeuser, H., Spielhagen, R.F., 2003. Stable isotope ratios in bivalve shells: suitable recorders for salinity and nutrient variability in the Kara Sea? In: Stein, R., Fahl, K., Fütterer, D.K., Galimov, E.M., Stepanets, O.V. (Eds.), Siberian River Run-off in the Kara Sea: Characterisation, Quantification, Variability, and Environmental Significance. Proceedings in Marine Sciences, vol. 6. Elsevier, Amsterdam, pp. 111–124.

Stein, R., Stepanets, O. (Eds.), 2000. Scientific Cruise Report of the Joint Russian–German Kara-Sea Expedition of RV "Akademik Boris Petrov" in 1999. Berichte zur Polarforschung—Reports on Polar Research 360. 141 pp.

Stein, R., Stepanets, O. (Eds.), 2001. The German–Russian Project on Siberian River Run-off (SIRRO): Scientific Cruise Report of the Kara-Sea Expedition "SIRRO 2000" of RV "Akademik Boris Petrov" and first results. Berichte zur Polar- und Meeresforschung—Reports on Polar and Marine Research 393. 287 pp.

Stein, R., Stepanets, O. (Eds.), 2002. Scientific Cruise Report of the Kara-Sea Expedition 2001 of RV "Akademik Boris Petrov": the German–Russian Project on Siberian River Run-off (SIRRO) and the EU Project "ESTABLISH". Reports on Polar and Marine Research, vol. 419. Alfred Wegener Institute for Polar and Marine Research, Bremerhaven. 278 pp.

Stein, R., Niessen, F., Dittmers, K., Levitan, M., Schoster, F., Simstich, J., Steinke, T., Stepanets, O.V., 2002. Siberian river run-off and Late Quaternary glaciation in the southern Kara Sea, Arctic Ocean: preliminary results. Polar Research 21 (2), 315–322.

Stein, R., Fahl, K., Dittmers, K., Niessen, F., Stepanets, O., 2003. Holocene siliciclastic and organic carbon fluxes in the Ob and Yenisei estuaries and the adjacent inner Kara Sea: quantification, variability, and paleoenvironmental implications. In: Stein, R., Fahl, K., Fütterer, D.K., Galimov, E.M., Stepanets, O.V. (Eds.), Siberian River Run-off in the Kara Sea: Character-

isation, Quantification, Variability, and Environmental Significance. Proceedings in Marine Sciences, vol. 6. Elsevier, Amsterdam, pp. 401–434.

Stepanova, A., Taldenkova, E., Bauch, H.A., 2003. Recent ostracoda from the Laptev Sea (Arctic Siberia): species assemblages and some environmental relationships. Marine Micropaleontology 48 (1–2), 23–48.

Stuiver, M., Reimer, P.J., 1993. Extended ^{14}C data base and revised CALIB 3.0 14C ages calibration program. Radiocarbon 35 (1), 215–230.

Svendsen, J.I., Alexanderson, H., Astakhov, V.I., Demidov, I., Dowdeswell, J.A., Funder, S., Gataullin, V., Henriksen, M., Hjort, C., Houmark-Nielsen, M., Hubberten, H.W., Ingólfsson, Ó., Jakobsson, M., Kjær, K.H., Larsen, E., Lokrantz, H., Lunkka, J.P., Lyså, A., Mangerud, J., Matioushkov, A., Murray, A., Möller, P., Niessen, F., Nikolskaya, O., Polyak, L., Saarnisto, M., Siegert, C., Siegert, M.J., Spielhagen, R.F., Stein, R., 2004. Late Quaternary ice sheet history of northern Eurasia.

Quaternary Science Reviews, in press.

Urey, H.C., Lowenstam, H.A., Epstein, S., McKinney, C.R., 1951. Measurements of paleotemperatures and temperatures of the Upper Cretaceous of England, Denmark and the southeastern United States. Bulletin of the Geological Society of America 62, 399–416.

Volkov, V.A., Johannessen, O.M., Borodachev, V.E., Voinov, G.N., Pettersson, L.H., Bobylev, L.P., Kouraev, A.V., 2002. Polar Seas Oceanography—An Integrated Case Study of the Kara Sea. Springer Verlag, Berlin. 450 pp.

Winsor, P., Chapman, D.C., 2002. Distribution and interannual variability of dense water production from coastal polynyas on the Chukchi Shelf. Journal of Geophysical Research 107 (C7), 3079 (doi:10.1029/2001JC000984).

Xia, J., Engstrom, D.R., Ito, E., 1997. Geochemistry of ostracode calcite: Part 2. The effects of water chemistry and seasonal temperature variation on *Candona rawsoni*. Geochimica et Cosmochimica Acta 61 (2), 383–391.